

ORIGINAL ARTICLE

Regional climate modeling in the Amazon basin to evaluate fire risk

Josivaldo Lucas Galvão SILVA^{1,2,*} , Vinicius Buscioli CAPISTRANO^{2,3}, José Augusto Paixão VEIGA³, Adriane Lima BRITO¹

¹ Instituto Nacional de Pesquisas da Amazônia (INPA), Programa de Pós Graduação em Clima e Ambiente (CLIAMB), Av. André Araújo 2936, Manaus, Amazonas, Brazil

² Universidade Federal do Mato Grosso do Sul, Cidade Universitária, Campo Grande, Mato Grosso do Sul, Brazil

³ Universidade do Estado do Amazonas (UEA), Av. Darcy Vargas 1200, Manaus, Amazonas, Brazil

* Corresponding author: lucas.sglv@gmail.com;  <https://orcid.org/0000-0003-0665-3785>

ABSTRACT

Studies regarding deforestation, the hydrological cycle, climate change and fire weather can benefit from the detailed simulations provided by regional climate models (RCM). While much attention has been given to fire activity in the Amazon, few studies have used RCM runs to assess fire risk and variables associated to fire occurrence. We evaluated precipitation, temperature and a fire risk index from the ensemble of Eta model simulations coupled with three different global climate models for the Amazon basin. The RCM runs were compared to reanalysis data for the dry season from 1979 to 2005. The maximum and 2-m temperature fields were underestimated over the entire region, but showed a statistically significant spatial correlation with the reference data. Precipitation was overestimated over the Amazon, in accordance with the major sources of moisture analyzed. The Keetch-Byram drought index (KBDI) was not significantly affected by the bias found in temperature and precipitation, and the ensemble improved relative to the individual member simulations. KBDI estimations performed better with the ensemble of the three evaluated members, however the Eta model showed some limitations. The validation of modeled fire risk could benefit from the use of satellite hotspot data. Furthermore, the KBDI can also be used in the assessment of how climate change interacts with fire activity in the Amazon region.

KEYWORDS: KBDI, Eta model, model validation, climate downscaling

Modelagem climática regional na bacia Amazônica para avaliação do risco de fogo

RESUMO

Estudos sobre desmatamento, ciclo hidrológico, mudanças climáticas e fogo podem se beneficiar de simulações mais detalhadas provenientes de modelos climáticos regionais (RCM). Apesar de que a atividade do fogo na Amazônia tenha recebido grande atenção, poucos estudos usaram simulações de RCM para avaliar o risco de fogo e variáveis associadas às condições climáticas favoráveis à ocorrência de fogo. Aqui avaliamos precipitação, temperatura e um índice de risco de fogo do conjunto de simulações do modelo Eta forçado para três modelos climáticos globais diferentes para a bacia Amazônica. As simulações de RCM foram comparadas com dados de reanálise para a estação seca de 1979 a 2005. Os campos de temperatura máxima e de 2 m foram subestimados em toda a região, porém mostraram uma correlação espacial estatisticamente significativa com os dados de referência. A precipitação foi superestimada para toda a Amazônia, em acordo com as principais fontes de umidade analisadas. O índice de seca de Keetch-Byram (KBDI) não foi significativamente afetado pelo viés observado na temperatura e na precipitação, e o conjunto apresentou resultados melhores em comparação com as simulações dos membros individuais. As simulações de KBDI tiveram melhor resultado com o conjunto das três variáveis avaliadas, porém o modelo Eta mostrou algumas limitações. A validação dos modelos de risco de fogo poderia se beneficiar do uso de dados de *hotspot* satelitais. Além disso, o KBDI pode ser usado na avaliação de como as mudanças climáticas interagem com o fogo na região amazônica.

PALAVRAS-CHAVE: KBDI, modelo Eta, validação de modelo, downscaling climático

INTRODUCTION

Global climate models (GCM) are a powerful tool for simulation of present and future climate. In order to function on a global scale, GCMs generally simulate the climate on a horizontal grid of 100-200 km, not allowing to represent some land, land-use, land-ocean and urban features, among others (Ambrizzi *et al.* 2019). Thus, a GCM has limitations such as the inability to simulate at a high level of detail, the lack of representation of small-scale processes and detailed near-surface variables (Cabr e *et al.* 2014). One way of surpassing this limitation is to use a regional climate model (RCM) with increased spatial resolution over a smaller domain, forcing it with lateral boundary conditions given by GCMs (Dickinson *et al.* 1989). Therefore, RCMs can be used as a multipurpose tool for studies that need a higher horizontal resolution (Xuejie *et al.* 2001; Campbell *et al.* 2011; Karmalkar *et al.* 2011; Van Oldenborgh *et al.* 2013; De Jong *et al.* 2019).

Due to their resolution, RCMs are expected to be able to represent meso-scale events. The detailed simulation can better represent the spatial and temporal variation of meteorological variables, such as short-duration phenomena, extreme events, small-scale events, cumulus convection, cloud-radiation forcing, and the influence of orography, land-sea and other surface interactions (Wang *et al.* 2004; Rummukainen *et al.* 2016). In the Amazon, regional models have already been used to validate the present climate (Chou *et al.* 2012; Builes-Jaramillo and P antano 2021), to simulate the effects of deforestation on regional circulation (Ruiz-V asquez *et al.* 2020; De Sales *et al.* 2020) and the hydrological cycle (Gomes *et al.* 2020), as well as to study climate change (Llopart *et al.* 2014; Rocha *et al.* 2015). Detailed simulations of precipitation and temperature can improve the quality of the assessment of changes in climate and the hydrological cycle through representation of changes in regional circulation (Ambrizzi *et al.* 2019). However, while there are some studies for fire weather and fire risk on a global scale (Liu *et al.* 2010; Fonseca *et al.* 2019; Gannon and Steinberg 2021), there is a lack of such studies on a regional scale, including the Amazon region. In the face of climate change scenarios, favorable conditions for fire occurrence may increase in the Amazon basin (Marengo *et al.* 2018; Vogel *et al.* 2020). This is particularly important since the Amazon rainforest stores 86 Pg carbon, and almost 80% of this biomass is above ground (Saatchi *et al.* 2007). When burned, the Amazon rainforest becomes a significant source of carbon for the atmosphere (Nobre and Borma 2009; Balch 2014; Gatti *et al.* 2021). Therefore, it is essential to understand the relationship between climate conditions and fire in the Amazon.

The vulnerability of the Amazon Forest to fires is enhanced by drought events (Arag ao *et al.* 2014), and this impact has been exacerbated over the years (Anderson *et al.* 2018). Drought events have a direct impact on carbon emission,

which was observed in the 2010, 2015 and 2016 droughts, when anomalous fires in the Amazon were responsible for a combined emission of 0.74 Pg CO₂ (Silva Junior *et al.* 2019). Moreover, the high spatial variability in precipitation during the drought season affects the distribution of fires in the Amazon basin (Carvalho *et al.* 2021). As climate change is further affecting precipitation variability and fire occurrence in the Amazon, it becomes increasingly necessary to understand fire dynamics and how it affects the accuracy of simulated fire risk on the regional scale, to understanding the uncertainties that climate models may carry to future climate scenarios.

We aimed to evaluate the physical processes related to optimal meteorological conditions for fire occurrence in the Amazon basin and the applicability of one fire risk index for climate change studies from the regional Eta climate model driven by three global climate models. We estimated the errors and uncertainties of simulations for the present climate during the Amazonian dry period (July, August and September), as well as the model's ability to represent the fire risk index.

MATERIAL AND METHODS

Study region

The Amazon basin is the largest hydrographic basin in the world, covering approximately 6.2 million km² and encompasses about 40% of the Brazilian territory, as well as parts of Bolivia, Colombia, Ecuador, Guyana, French Guiana, Peru, Suriname and Venezuela. The average annual accumulated rainfall in the region is approximately 2,300 mm year⁻¹ and average temperatures vary between 24 °C and 26 °C, with low thermal amplitude throughout the year (Fisch *et al.* 1998). One of the defining characteristics of the region is the high spatial and temporal variability of rainfall (Sombroek 2001; Espinoza-Villar *et al.* 2009), due to the atmospheric systems that act over the region, such as the intertropical convergence zone (Mehta 1998; Wang and Fu 2007), the South Atlantic convergence zone (Kodama 1992), the Bolivian high (Lenters and Cook 1997), the Pacific decadal oscillation and the El Ni o-Southern Oscillation (Marengo 2004; Espinoza-Villar *et al.* 2009).

Regional circulation model

The regional climate model used for this study was the Eta model (Black 1994). One of the main features of the Eta regional model is the Eta vertical coordinate (η), defined by Mesinger (1984), which reduces the error in calculations near steep surfaces of variables such as the strength of the pressure gradient, advective processes and horizontal diffusion (Dereczynski *et al.* 2000). The Eta model uses Arakawa's E-type horizontal grid (Arakawa and Lamb 1977) and, for this study, it was configured with a horizontal resolution of 20 km and 38 vertical levels.

For the simulations, the Eta model used the parametrization of turbulent diffusion in the planetary boundary layer proposed by Mellor and Yamada (1974). Shortwave radiation (Fels and Schwarzkopf 1975) and longwave radiation (Lacis and Hansen 1974) parametrizations are present. In addition, cumulus parametrization using the Betts-Miller-Janjic scheme (Janjić 1994) and cloud microphysics (Zhao *et al.* 1997) are used to simulate precipitation. Land processes are represented by the NOAA land surface model (LSM) (Ek *et al.* 2003). The NOAA model uses four soil layers, 13 vegetation covers and nine different soil types (Hogue *et al.* 2005). Since the surface layer of the LSM is a combination of the soil and vegetation surface, it is not possible to explicitly calculate some variables such as canopy temperature, carbon fluxes and photosynthetically radiation. However, the LSM has been fitted with various enhancements throughout the years, for canopy conductance soil evaporation, vegetation phenology, surface runoff, infiltration and others (Ek *et al.* 2003 and references therein). For this simulation, the category of broadleaf-evergreen tree was used to represent the tropical forest, and cultivations to represent deforested areas.

To perform the simulations, the Eta regional model was adapted to use the monthly averages of sea surface temperature (SST) provided by the earth system models (BESM, HadGEM2-ES and MIROC5), to use a 360-day year calendar, in order for the Eta model to be compatible with the HadGEM2-ES lateral boundary conditions.

Earth system models

The Brazilian Earth System Model (BESM) is an earth system model built from a national effort aimed at understanding global climate change, its causes, effects, and impacts on society (Nobre *et al.* 2013; Capistrano *et al.* 2020). It was set up at a horizontal resolution of approximately 200 km and 28 vertical levels. In order to represent atmospheric and land surface processes, BESM uses the Brazilian Atmospheric Model (BAM) (Figueroa *et al.* 2016) and the Simplified Simple Biosphere Model - SSiB (Xue *et al.* 2001), respectively. The shortwave radiation calculation is based on the CLIRAD-SW-M model (Tarasova *et al.* 2007), and the Harshvardhan *et al.* (1987) scheme calculates the longwave radiation. The cloud interaction is based on the scheme described in Slingo (1987), Hou (1990) and Kinter *et al.* (1997).

The UK Met Office Hadley Centre Global Environmental Model, version 2 (HadGEM2-ES) is an earth system model (Collins *et al.* 2011). The horizontal resolution of the atmospheric component is N96, approximately 1.875° x 1.25°, with 38 vertical levels. The global dynamic vegetation model TRIFFID (top-down representation of interactive foliage including dynamics) (Cox 2001) was used to describe the terrestrial vegetation and carbon cycle. Oceanic biological and chemical processes were represented by the DiatHadOCC model (Halloran *et al.* 2010). The UKCA model (United

Kingdom Chemistry and Aerosol model) was used to calculate the chemistry of the troposphere.

The Model for Interdisciplinary Research on Climate (MIROC), version 5 is described in detail by Watanabe *et al.* (2010). The atmospheric spectral component of the model has T85 resolution, which corresponds to approximately 150 km horizontally and has 40 vertical levels. The ocean coupling was performed using the COCO 4.5 model, which has 1° of resolution horizontally and 50 depth levels. The radiative transfers are calculated using the k distribution scheme (Sekiguchi and Nakajima 2008). The model has a cloud microphysics scheme that is coupled with the radiation scheme, and is called SPRINTARS. To represent surface processes MIROC5 uses the MATSIRO scheme (Takata *et al.* 2003).

Model description and simulation strategy

In this study, the Eta regional climate model, nested with three different earth system models (ESMs), was used to simulate the present climate. The three runs were performed for the period 1960 to 2005, using the initial and boundary conditions of the Brazilian Earth System Model (BESM), the UK Met Office Hadley Centre Global Environmental Model (HadGEM2-ES) and the model for Interdisciplinary Research on Climate (MIROC5). This Eta configuration with Coupled Model Intercomparison Project Phase 5 (CMIP5) models was chosen as it has already assessed South America's historical climate (Chou *et al.* 2014) and also was used in climate change assessments (Brito *et al.* 2022). The models ran continuously throughout the 45 years, initiating at 00:00 GMT of January 1st, 1960, in 10-minute time-steps. Precipitation and temperature were given by the model in 6-hour frequency, and later re-calculated to a daily scale. Levels of CO₂ were fixed at 330 ppm. The vegetation map used in the Eta model was obtained from the ProVeg project (Sestini *et al.* 2002), and updated with deforestation data for the base year of 2015 from Projeto de Monitoramento do Desmatamento da Floresta Amazônica Brasileira por Satélite – PRODES (INPE 2023).

Fire risk index

The Keetch-Byram drought index (KBDI) was used to estimate soil moisture through precipitation and maximum daily temperature. Since soil moisture deficiency and droughts can influence the flammability of vegetation, the KBDI is used as a tool for identifying dry areas that are susceptible to the occurrence of wildfires (Keetch and Byram 1968). The KBDI has been applied in tropical areas (Dolling *et al.* 2005; Taufik *et al.* 2015) and specifically in the Amazon biome, with statistically significant results for predicting fire occurrence (Nogueira *et al.* 2017; Cavalcante *et al.* 2021). The main advantage of using this index is that it only requires two meteorological variables (daily maximum temperature and

daily precipitation). It gives values ranging from 0, when there is no soil moisture deficiency, to 800, which denotes absolute soil moisture deficiency (Heim 2002). KBDI values correlate to fire risk in a scale where values from 0 to 200 correspond to low risk, 200 to 400 to moderate risk, 400 to 600 to high risk, and 600 to 800 to very high risk (Liu *et al.* 2010).

The KBDI is calculated according to equations 1 and 2, with variables expressed following the international unit system (Crane 1982):

$$KBDI_t = KBDI_{t-1} + dQ - dP \quad [1]$$

$$dQ = \frac{[203.2 - KBDI][0.968 \exp(0.0875T + 1.5552) - 8.30]dt}{1 + 10.88 \exp(-0.001736R)} \times 10^{-3} \quad [2]$$

where dP is the daily precipitation (mm), dQ is the drought factor (mm), KBDI is the moisture deficiency in mm, T is the maximum daily temperature ($^{\circ}C$), dt is the time variation, which equals to one day, and R is the average annual precipitation in mm.

Observed data and model validation

The NOAA Climate Prediction Center’s (CPC) precipitation and maximum temperature dataset (Xie *et al.* 2010) was used to assess the ensemble of the Eta simulations with an integration period of 1979-2005, as the CPC dataset begins on January 1979. The CPC dataset is available at a regular spatial resolution of 0.50 x 0.50 degrees. The KBDI, which was calculated with precipitation and maximum temperature simulated by the Eta model, was compared against the KBDI calculated by the same variables from the CPC dataset. Similarly, the simulated near-surface temperature was evaluated using the European Centre for Medium-Range Weather Forecasts (ECMWF) ERA5 monthly reanalysis data at 0.25 degrees (Hersbach *et al.* 2020). Maximum temperature was chosen for validation of the regional model because it is one of the most important meteorological variables for

fire occurrence. Precipitation was evaluated as it is a natural barrier against fire occurrence and spread. Also, in order to understand how well the model simulates long periods without precipitation and how it impacts the fire risk, we also calculated the number of consecutive dry days (CDD) with a 1mm precipitation threshold. The validation took place over the dry period (July, August and September), using a three-member ensemble (Eta-BESM, Eta-HadGEM2-ES, Eta-MIROC5). For comparison, the bias method was used on mean values and, in order to evaluate the pattern between the reference and simulations, the Taylor diagram (Taylor 2001) was used.

RESULTS

Near-surface temperature

The southern part of the Amazon basin is the area where the models simulated the warmest temperature at 2 m. However, the ensemble models also show a cold bias in the northern and western areas of the basin (Figure 1a). The positive bias was mainly due to the Eta-BESM run (Supplementary Material, Figure S1a), which overestimated the temperature in the entire basin with the exception of the Andes region. On the other hand, Eta-MIROC5 presented the greatest cold bias among the members of the ensemble, although Eta-HadGEM2-ES also demonstrates a cold bias for the northern, western and central regions of the Amazon basin (Supplementary Material, Figures S1b and S1c, respectively). The Taylor diagram shows that all simulations of the Eta model are very close to each other (Figure 1b), indicating that, even when forced with different initial and boundary conditions, all simulations result in a very close temperature pattern output. In addition, the simulations showed high spatial correlation with the reference data, the highest for the Eta-HadGEM2-ES simulation (0.97). The ensemble correlation (0.96) was the

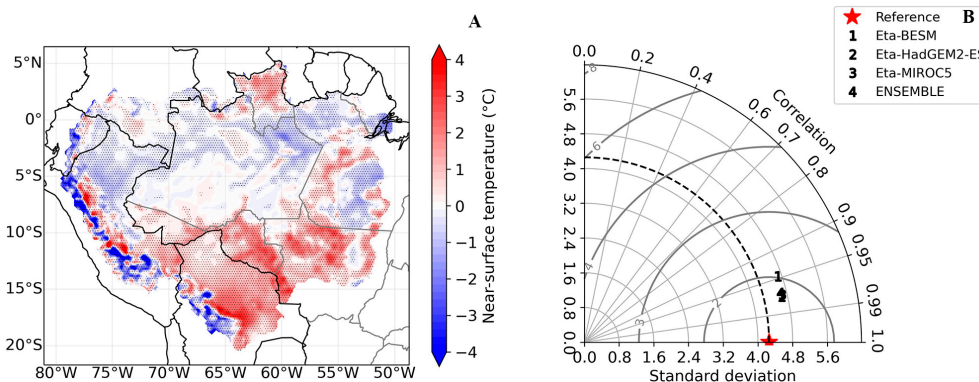


Figure 1. A – Near-surface temperature bias ($^{\circ}C$) from ERA5 versus the ensemble for the dry period (July, August and September) in the Amazon basin from 1979 to 2005. Dotted regions are statistically significant at a 95% confidence level. B – Taylor diagram of the near-surface temperature ($^{\circ}C$) for the dry period (July, August and September) in the Amazon basin from 1979 to 2005. The points from 1 to 4 are the different climate simulations and the red star is the reference data. This figure is in color in the electronic version..

second best, showing an improvement over the Eta-BESM and Eta-MIROC5 runs.

Maximum temperature

The ensemble's cold bias is present throughout the study area (Figure 2a), i.e., the simulations tended to underestimate the maximum temperature in the dry period. The cold bias was lowest in the southeast and northwest of the basin and, consequently, the uncertainty in the simulation is greater there. The Eta model also produced a significant cold bias in the region near the Andes. While the Eta-BESM run (Supplementary Material, Figure S2a) showed a distinct pattern from the Eta-HadGEM2-ES run (Supplementary Material, Figure S2b), which simulated the largest underestimation of maximum temperatures, it had close agreement with the Eta-MIROC5 run (Supplementary Material, Figure S2c). The difference between the standard deviation from the reference data (3.2) and the simulation (approximately 4.8) is a direct consequence of the bias found (Figure 2b). Although the simulations do not show high dispersion among simulated and reference values in the Taylor diagram, the simulated temperature pattern differs

from the reference by more than 2 °C. However, as with the near-surface temperature, there was high spatial correlation between reference and simulated maximum temperature, the highest with the three-member ensemble (0.92) and the lowest with Eta-BESM (0.89).

Precipitation

Precipitation was overestimated for this period in almost the entire basin (Figure 3a), with the highest positive bias in the west, over the Andes, with an overestimation of approximately 7 mm day⁻¹. The overestimation of precipitation is not unique to the Andes, extending to almost the entire area. The Eta-BESM and Eta-HadGEM2-ES simulations showed similar behavior by simulating more than the observed precipitation (Supplementary Material, Figures S3a and S3b), with highest overestimation for Eta-BESM, concentrated in the central and western basin. The Eta-MIROC5, in turn, resulted in more areas with negative (dry) bias (Supplementary Material, Figure S3c) and was the closest to the observed precipitation pattern, as the south of the basin is drier in July-August-September, with higher precipitation in the central and northern regions.

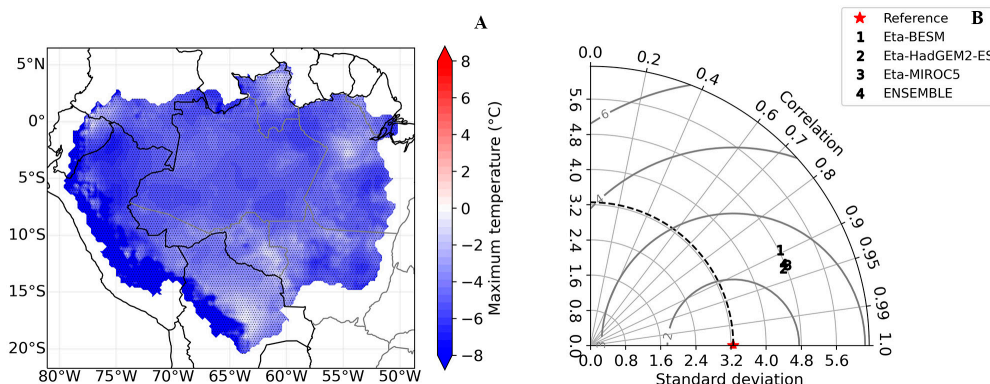


Figure 2. A – Maximum temperature bias (°C) from CPC versus the ensemble, for the dry period (July, August and September) in the Amazon basin from 1979 to 2005. Dotted regions are statistically significant at a 95% confidence level. B – Taylor diagram of the maximum temperature (°C) for the dry period (July, August and September) in the Amazon basin from 1979 to 2005. The points from 1 to 4 are the different climate simulations and the red star is the reference data. This figure is in color in the electronic version.

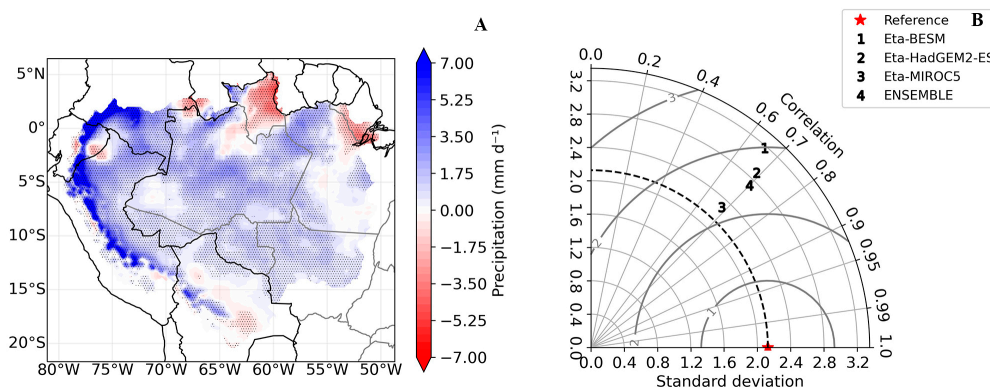


Figure 3. A – Precipitation bias (mm d⁻¹) from CPC versus ensemble, for the dry period (July, August and September) in the Amazon basin from 1979 to 2005. Dotted regions are statistically significant at a 95% confidence level. B – Taylor diagram of the precipitation (mm d⁻¹) for the dry period (July, August and September) in the Amazon basin from 1979 to 2005. The points from 1 to 4 are the different climate simulations and the red star is the reference data. This figure is in color in the electronic version.

In the Taylor diagram, the precipitation pattern simulated by Eta-BESM deviated more from the observed (reference) values (Figure 3b). Among the four simulations, the ensemble had the highest correlation with the reference values (0.70).

Keetch-Byram drought index

The KBDI showed a well-defined spatial bias distribution (Figure 4b). The ensemble tended to overestimate the KBDI in the central and northern basin, with higher values concentrated in the northeastern sector. In the southeastern basin and in the west, near the Andes, the bias was negative. The simulated KBDI higher than the observed in the northern and central basin despite positive bias for precipitation and negative bias for maximum temperature in this region (Figures 2a and 3a). Even an overestimation of approximately 75 units in the KBDI in the northern region did not change the observed classification of fire risk (Figure 4a). The regions of low and high values for the KBDI calculated from the CPC dataset (Figure 4a) showed positive and negative bias, respectively (Figure 4b). The Eta-BESM run showed predominantly negative bias over the basin (Supplementary Material, Figure S4a, while the Eta-HadGEM2-ES run showed the highest

positive bias among the models, and overestimated the KBDI for the entire basin except the Andes (Supplementary Material, Figure S4b). The Eta-MIROC5 run (Supplementary Material, Figure S4c) behaved similarly to the ensemble.

The number of consecutive dry days (CDD) reached more than 40 days of positive bias in the far northeast of the basin, while it was underestimated over the west, near the Andes, and southeast (Figure 5a), where the KBDI was also underestimated.

The Taylor diagram for KBDI showed greatest dispersion among all variables (Figure 5b), reflecting the high variability of simulated KBDI patterns. The Eta-HadGEM2-ES simulation was the closest in standard deviations to the observed data and also showed the highest correlation with the reference values (0.70). The ensemble simulation (approximately 0.69) was very close to the Eta-HadGEM2-ES.

DISCUSSION

The simulations of the present climate have shown significant biases over the Amazon basin. The negative bias in near-surface temperature for the northern basin agrees

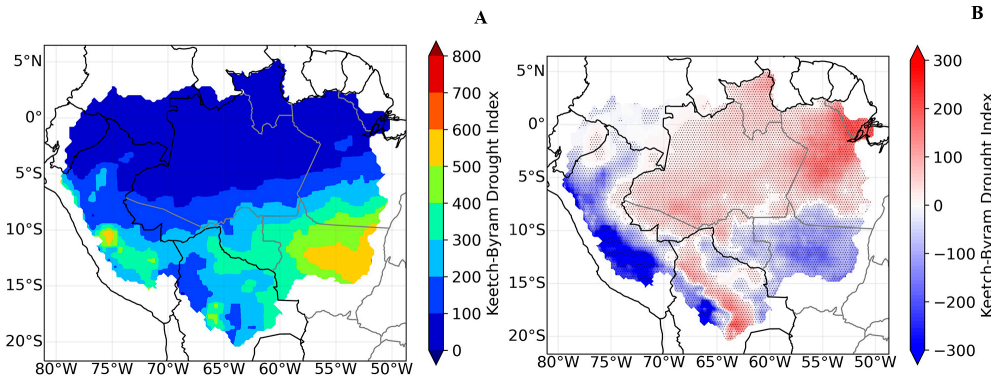


Figure 4. Keetch-Byram drought index calculated from the CPC dataset (A) and calculated from the CPC versus the ensemble data, for the dry period (July, August and September) in the Amazon basin from 1979 to 2005 (B). Dotted regions are statistically significant at a 95% confidence level. This figure is in color in the electronic version..

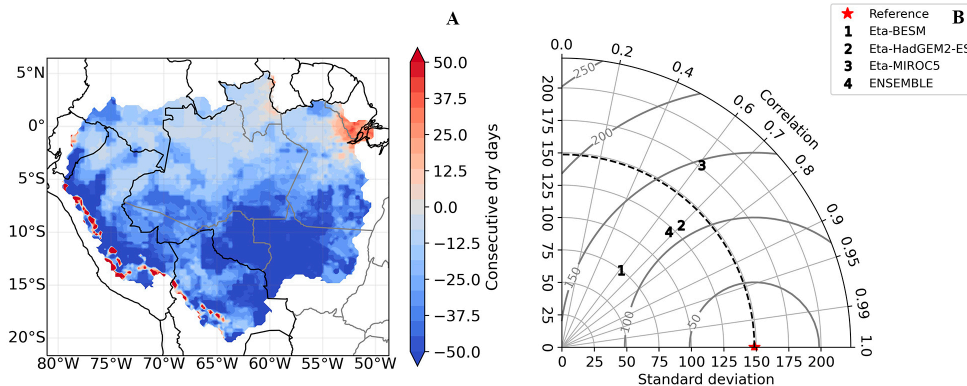


Figure 5. A – Consecutive dry days bias from the CPC versus ensemble, for the dry period in the Amazon basin (July, August and September) from 1979 to 2005. B – Taylor diagram of the Keetch-Byram drought index for the dry period in the Amazon basin (July, August and September) from 1979 to 2005. The points from 1 to 4 are the different climate simulations and the red star is the reference data. This figure is in color in the electronic version..

with previous simulations using the Eta regional model in the Amazon region. Pesquero *et al.* (2010) used the Eta model nested within the HadAM3P model and also found underestimation of near-surface temperatures in June, July and August from 1961 to 1970. These coincident patterns could indicate that the underestimation of near-surface temperatures is generated by the Eta model irrespective of its boundary conditions. Furthermore, the prominent negative bias over the Andes can be related to a model response to the topographic configuration and the simulation of high orographic precipitation. The presence of regions where the bias value showed values of zero or very close to zero, however, show that the three-member ensemble is able to improve the results of simulations using individual variables. Despite the uncertainties in the simulations, the Taylor diagrams indicated that the Eta model is able to satisfactorily represent the near-surface temperature in the dry period in the Amazon basin. The underestimation of maximum temperatures over the entire basin agrees with Chou *et al.* (2014), who found a negative bias for the northern region in both the austral winter and summer, highlighting the tendency of the Eta model to underestimate maximum temperatures for the northern Brazilian Amazon.

While there was an overestimation of precipitation for the entire basin, the bias was greater over the Andes. The presence of the Andes is one of the main driving factors of precipitation in the central and northwestern Amazon basin, as they cause upwards movement of moist air brought by the trade winds (Nobre *et al.* 1991). Our study confirms that the Eta simulations systematically generate errors in the Andes region, as already shown by Chou *et al.* (2012 and 2014), likely due to the lack of observational data for this region.

In the Amazon, around 32% of the precipitation originates from the basin itself (Staal *et al.* 2018), therefore the overestimation of local sources of moisture by the Eta model ensemble could lead to increased simulated rainfall. Two moisture sources for precipitation were analyzed to understand this positive bias in precipitation, namely the evapotranspiration and the P-E (precipitation minus evapotranspiration), which indicates the moisture flux convergence (Marengo *et al.* 2012). We found a positive bias in simulated evapotranspiration and positive values of P-E mean moisture convergence over the region and the P-E was also overestimated over the basin. The behavior of these two moisture sources could explain the bias found in the simulated precipitation, in addition to the errors over the Andes.

The KBDI was overestimated in the central and northern Amazon basin, and underestimated in the Andes and in the southeast. The KBDI considers maximum temperature, precipitation and the accumulation of a deficiency in soil moisture to calculate the fire risk, therefore weather conditions from previous months influence the period evaluated (Liu

et al. 2010). Our results suggest that the KBDI does not have a linear relationship with precipitation and maximum temperature. The bias pattern of the KBDI and the CDD were overlaid, as both were overestimated in the northeastern basin, and underestimated in the south. Likewise, in an Eta model forced by HadGEM2-ES for the period 1981-1990, CDD was overestimated in the northeastern region of the Amazon basin, and underestimated in the western and southern regions (Brito *et al.* 2019). Additionally, using the Eta model at 40 km resolution, Dereczynski *et al.* (2020) found that CDDs are reduced over the Amazon region. Thus, the nonlinear interactions among precipitation, temperature and CDD likely condition the biases found for the KBDI.

The ensemble simulations seemed to represent KBDI values more accurately at the center, with a poorer representation of the extremes of the variable distribution. The ensemble showed less bias compared to the individual members, suggesting that using the ensemble method can improve the representation of the index and mitigate uncertainties in the simulation of the individual members.

Fires in the Amazon Forest are heavily associated with deforestation and the process of slash-and-burning, when not used properly (Berenguer *et al.* 2014; Brando *et al.* 2014). As the KBDI only infers the fire risk through meteorological conditions (Gannon and Steinberg 2021), it may fail to identify areas that are more likely to present fire activity. While forest fragmentation, fuel and ignition are conditions for fire occurrence and spread (Nepstad 1999; Brando *et al.* 2019), the study of weather conditions that favor to fire activity is equally relevant, not only because fire activity increases in years of extreme drought in the Amazon (Aragão *et al.* 2014; Anderson *et al.* 2018; Silva Junior *et al.* 2019), but also because the Amazon forest is gradually losing its resilience to fire, such as the decrease in cold nights (Balch *et al.* 2022; Reboita *et al.* 2022).

CONCLUSIONS

The use of the Eta regional model over the Amazon basin to evaluate fire risk showed significant bias in all variables evaluated. The simulation using the ensemble of near-surface temperature, maximum temperature and precipitation showed improvements when compared to the simulations using individual members and, thus, is suggested as a method to better estimate the fire risk index and mitigate uncertainties in the simulations of the individual members. Our results indicate that the calculation of the KBDI in the Amazon basin is heavily dependent on how well the model simulate precipitation, more specifically the number of consecutive days without rainfall. The simplistic formulation of the KBDI facilitates its calculation and use for fire risk monitoring. In order to reduce the uncertainties of potential fire risk estimation over the region, the Eta model must improve

the simulation of the climate over the Andes and simulate more accurately the number of consecutive dry days over the entire Amazon region. Information on soil condition and the validation of the KBDI with satellite data on observed fires could increase the accuracy of the fire risk index in the Amazon basin.

ACKNOWLEDGMENTS

This study was developed in the Post-Graduate Program in Climate and Environment of Universidade do Estado do Amazonas and Instituto Nacional de Pesquisas da Amazônia (CLIAMB – UEA/INPA). We thank the Center for Weather Forecasting and Climate Studies – Instituto Nacional de Pesquisas Espaciais (CPTEC/INPE) for providing access to the supercomputer where the numerical integrations were performed, and the Laboratory of Terrestrial Climate System Modeling (LABCLIM) at UEA for providing the computational physical structure (ARUANÁ Cluster). The first author thanks the Conselho Nacional de Desenvolvimento Científico e Tecnológico (CNPq) for the master's grant GM/GD # 131459/2020-1.

REFERENCES

- Ambrizzi, T.; Reboita, M.S.; da Rocha, R.P.; Llopart, M. 2019. The state of the art and fundamental aspects of regional climate modeling in South America: Climate modeling in South America. *Annals of the New York Academy of Sciences*, 1436: 98–120.
- Anderson, L.O.; Ribeiro Neto, G.; Cunha, A.P.; Fonseca, M.G.; Mendes de Moura, Y.; Dalagnol, R.; et al. 2018. Vulnerability of Amazonian forests to repeated droughts. *Philosophical Transactions of the Royal Society B: Biological Sciences*, 373: 20170411.
- Aragão, L.E.O.C.; Poulter, B.; Barlow, J.B.; Anderson, L.O.; Malhi, Y.; Saatchi, S.; et al. 2014. Environmental change and the carbon balance of Amazonian forests: Environmental change in Amazonia. *Biological Reviews*, 89: 913–931.
- Arakawa, A.; Lamb, V.R. 1977. Computational design of the basic dynamical processes of the UCLA General Circulation Model. In: Chang, J. (Ed.). *Methods in Computational Physics: Advances in Research and Applications*, vl.17, Elsevier, Cambridge, p.173–265.
- Balch, J.K. 2014. Drought and fire change sink to source. *Nature*, 506: 41–42.
- Balch, J.K.; Abatzoglou, J.T.; Joseph, M.B.; Koontz, M.J.; Mahood, A.L.; McGlinchy, J.; et al. 2022. Warming weakens the nighttime barrier to global fire. *Nature*, 602: 442–448.
- Berenguer, E.; Ferreira, J.; Gardner, T.A.; Aragão, L.E.O.C.; De Camargo, P.B.; Cerri, C.E.; et al. 2014. A large-scale field assessment of carbon stocks in human-modified tropical forests. *Global Change Biology*, 20: 3713–3726.
- Black, T.L. 1994. The New NMC Mesoscale Eta Model: Description and Forecast Examples. *Weather and Forecasting*, 9: 265–278.
- Brando, P.M.; Balch, J.K.; Nepstad, D.C.; Morton, D.C.; Putz, F.E.; Coe, M.T.; et al. 2014. Abrupt increases in Amazonian tree mortality due to drought–fire interactions. *Proceedings of the National Academy of Sciences*, 111: 6347–6352.
- Brando, P.M.; Paolucci, L.; Ummenhofer, C.C.; Ordway, E.M.; Hartmann, H.; Cattau, M.E.; et al. 2019. Droughts, wildfires, and forest carbon cycling: A pantropical synthesis. *Annual Review of Earth and Planetary Sciences*, 47: 555–581.
- Brito, A.L.; Veiga, J.A.P.; Correia, F.W.; Capistrano, V.B. 2019. Avaliação do desempenho dos modelos HadGEM2-ES e Eta a partir de indicadores de extremos climáticos de precipitação para a Bacia Amazônica. *Revista Brasileira de Meteorologia*, 34: 165–177.
- Brito, A.; Veiga, J.; Correia, F.; Michiles, A.; Capistrano, V.; Chou, S.; et al. 2022. Impacts of greenhouse gases and deforestation in Amazon Basin climate extreme indices. *Climate Research*, 88: 39–56.
- Builes-Jaramillo, A.; Pántano, V. 2021. Comparison of spatial and temporal performance of two Regional Climate Models in the Amazon and La Plata river basins. *Atmospheric Research*, 250: 105413.
- Cabré, F.; Solman, S.; Núñez, M. 2014. Climate downscaling over southern South America for present-day climate (1970–1989) using the MM5 model. Mean, interannual variability and internal variability. *Atmósfera*, 27: 117–140.
- Campbell, J.D.; Taylor, M.A.; Stephenson, T.S.; Watson, R.A.; Whyte, F.S. 2011. Future climate of the Caribbean from a regional climate model. *International Journal of Climatology*, 31: 1866–1878.
- Capistrano, V.B.; Nobre, P.; Veiga, S.F.; Tedeschi, R.; Silva, J.; Bottino, M.; et al. 2020. Assessing the performance of climate change simulation results from BESM-OA2.5 compared with a CMIP5 model ensemble. *Geoscientific Model Development*, 13: 2277–2296.
- Carvalho, N.S.; Anderson, L.O.; Nunes, C.A.; Pessôa, A.C.M.; Silva Junior, C.H.L.; Reis, J.B.C.; et al. 2021. Spatio-temporal variation in dry season determines the Amazonian fire calendar. *Environmental Research Letters*, 16: 125009.
- Cavalcante, R.B.L.; Souza, B.M.; Ramos, S.J.; Gastauer, M.; Nascimento Junior, W.R.; Caldeira, C.F.; et al. 2021. Assessment of fire hazard weather indices in the eastern Amazon: a case study for different land uses. *Acta Amazonica*, 51: 352–362.
- Chou, S.C.; Marengo, J.A.; Lyra, A.A.; Sueiro, G.; Pesquero, J.F.; Alves, L.M.; et al. 2012. Downscaling of South America present climate driven by 4-member HadCM3 runs. *Climate Dynamics*, 38: 635–653.
- Chou, S.C.; Lyra, A.; Mourão, C.; Dereczynski, C.; Pilotto, I.; Gomes, J.; et al. 2014. Evaluation of the Eta simulations nested in three global climate models. *American Journal of Climate Change*, 3: 438–454.
- Collins, W.J.; Bellouin, N.; Doutriaux-Boucher, M.; Gedney, N.; Halloran, P.; Hinton, T.; et al. 2011. Development and evaluation of an Earth-System model – HadGEM2. *Geoscientific Model Development*, 4: 1051–1075.
- Cox, P.M. 2001. Description of the “TRIFFID” dynamic global vegetation model. Hadley Centre Technical Note #24,

- Met Office, UK. (https://jules.jchmr.org/sites/default/files/HCTN_24.pdf). Accessed on 02 Jan 2023.
- Crane, W.J.B. 1982. Computing grassland and forest fire behavior, relative humidity and drought index by pocket calculator. *Australian Forestry*, 45: 89–97.
- de Jong, P.; Barreto, T.B.; Tanajura, C.A.S.; Kouloukoui, D.; Oliveira-Esquerre, K.P.; Kiperstok, A.; et al. 2019. Estimating the impact of climate change on wind and solar energy in Brazil using a South American regional climate model. *Renewable Energy*, 141: 390–401.
- De Sales, F.; Santiago, T.; Biggs, T.W.; Mullan, K.; Sills, E.O.; Monteverde, C. 2020. Impacts of protected area deforestation on dry-season regional climate in the Brazilian Amazon. *Journal of Geophysical Research: Atmospheres*, 125: e2020JD033048.
- Dereczynski, C.P.; Rozante, J.R.; Chou, S.C. 2000. Avaliação do desempenho do modelo regional ETA utilizando uma topografia de 30 segundos. In: Proceedings of the 11th Congresso Brasileiro de Meteorologia, Rio de Janeiro. p.1599-1608. (<http://mtc-m16b.sid.inpe.br/rep/cptec.inpe.br/walmeida/2004/05.27.08.03?ibiurl.backgroundlanguage=pt-BR>). Accessed on 02 Feb 2023
- Dereczynski, C.; Chan Chou, S.; Lyra, A.; Sondermann, M.; Regoto, P.; Tavares, P.; et al. 2020. Downscaling of climate extremes over South America – Part I: Model evaluation in the reference climate. *Weather and Climate Extremes*, 29: 100273.
- Dickinson, R.E.; Errico, R.M.; Giorgi, F.; Bates, G.T. 1989. A regional climate model for the western United States. *Climatic Change*, 15: 383–422.
- Dolling, K.; Chu, P.-S.; Fujioka, F. 2005. A climatological study of the Keetch/Byram drought index and fire activity in the Hawaiian Islands. *Agricultural and Forest Meteorology*, 133: 17–27.
- Ek, M.B.; Mitchell, K.E.; Lin, Y.; Rogers, E.; Grunmann, P.; Koren, V.; et al. 2003. Implementation of Noah land surface model advances in the National Centers for Environmental Prediction operational mesoscale Eta model. *Journal of Geophysical Research: Atmospheres*, 108: 2002JD003296.
- Espinoza Villar, J.C.; Ronchail, J.; Guyot, J.L.; Cochonneau, G.; Naziano, F.; Lavado, W.; et al. 2009. Spatio-temporal rainfall variability in the Amazon basin countries (Brazil, Peru, Bolivia, Colombia, and Ecuador). *International Journal of Climatology*, 29: 1574–1594.
- Fels, S.B.; Schwarzkopf, M.D. 1975. The simplified exchange approximation: A new method for radiative transfer calculations. *Journal of the Atmospheric Sciences*, 32: 1475–1488.
- Figueroa, S.N.; Bonatti, J.P.; Kubota, P.Y.; Grell, G.A.; Morrison, H.; Barros, S.R.M.; et al. 2016. The Brazilian Global Atmospheric Model (BAM): Performance for tropical rainfall forecasting and sensitivity to convective scheme and horizontal resolution. *Weather and Forecasting*, 31: 1547–1572.
- Fisch, G.; Marengo, J.A.; Nobre, C.A. 1998. Uma revisão geral sobre o clima da Amazônia. *Acta Amazonica*, 28: 101–126.
- Fonseca, M.G.; Alves, L.M.; Aguiar, A.P.D.; Arai, E.; Anderson, L.O.; Rosan, T.M.; et al. 2019. Effects of climate and land-use change scenarios on fire probability during the 21st century in the Brazilian Amazon. *Global Change Biology*, 25: 2931–2946.
- Gannon, C.S.; Steinberg, N.C. 2021. A global assessment of wildfire potential under climate change utilizing Keetch-Byram drought index and land cover classifications. *Environmental Research Communications*, 3: 035002.
- Gatti, L.V.; Basso, L.S.; Miller, J.B.; Gloor, M.; Gatti Domingues, L.; Cassol, H.L.G.; et al. 2021. Amazonia as a carbon source linked to deforestation and climate change. *Nature*, 595: 388–393.
- Gomes, W.; Correia, F.; Capistrano, V.; Veiga, J.; Vergasta, L.; Chou, S.; et al. 2020. Water budget changes in the Amazon basin under RCP 8.5 and deforestation scenarios. *Climate Research*, 80: 105–120.
- Halloran, P.R.; Bell, T.G.; Totterdell, I.J. 2010. Can we trust empirical marine DMS parameterisations within projections of future climate? *Biogeosciences*, 7: 1645–1656.
- Harshvardhan; Davies, R.; Randall, D.A.; Corsetti, T.G. 1987. A fast radiation parameterization for atmospheric circulation models. *Journal of Geophysical Research*, 92: 1009-1016.
- Heim, R.R. 2002. A Review of twentieth-century drought indices used in the United States. *Bulletin of the American Meteorological Society*, 83: 1149–1166.
- Hersbach, H.; Bell, B.; Berrisford, P.; Hirahara, S.; Horányi, A.; Muñoz-Sabater, J.; et al. 2020. The ERA5 global reanalysis. *Quarterly Journal of the Royal Meteorological Society*, 146: 1999–2049.
- Hogue, T.S.; Bastidas, L.; Gupta, H.; Sorooshian, S.; Mitchell, K.; Emmerich, W. 2005. Evaluation and transferability of the Noah Land Surface Model in semiarid environments. *Journal of Hydrometeorology*, 6: 68–84.
- Hou, Y. 1990. *Cloud-Radiation Dynamics Interaction*. PhD thesis, University of Maryland, USA, 209p.
- INPE. 2023. PRODES - Desflorestamento nos Municípios - DPI/INPE. (<http://www.dpi.inpe.br/prodesdigital/prodesmunicipal.php>). Accessed on 04 Feb 2023.
- Janjić, Z.I. 1994. The step-mountain Eta coordinate model: Further developments of the convection, viscous sublayer, and turbulence closure schemes. *Monthly Weather Review*, 122: 927–945.
- Karmalkar, A.V.; Bradley, R.S.; Diaz, H.F. 2011. Climate change in Central America and Mexico: regional climate model validation and climate change projections. *Climate Dynamics*, 37: 605–629.
- Keetch, J.J.; Byram, G.M.A. 1968. *Drought Index for Forest Fire Control*. Research Paper SE-38. US Department of Agriculture, Forest Service, Southeastern Forest Experiment Station, Asheville, 35p.
- Kinter, J.L.; DeWitt, D.; Dirmeyer, P.A.; Fennessy, M.J.; Kirtman, B.P.; Marx, L.; Schneider, E.K.; Shukla, J.; Straus, D.M. 1997. *The COLA Atmosphere-Biosphere General Circulation Model, v.1*. Rep. 51, COLA, Calverton, 46p.
- Kodama, Y. 1992. Large-scale common features of subtropical precipitation zones (the Baiu Frontal Zone, the SPCZ, and the SACZ), Part I: Characteristics of subtropical frontal zones. *Journal of the Meteorological Society of Japan. Ser. II*, 70: 813–836.
- Lacis, A.A.; Hansen, J. 1974. A parameterization for the absorption of solar radiation in the Earth's atmosphere. *Journal of the Atmospheric Sciences*, 31: 118–133.

- Lenters, J.D.; Cook, K.H. 1997. On the origin of the Bolivian high and related circulation features of the South American climate. *Journal of the Atmospheric Sciences*, 54: 656–678.
- Liu, Y.; Stanturf, J.; Goodrick, S. 2010. Trends in global wildfire potential in a changing climate. *Forest Ecology and Management*, 259: 685–697.
- Llopart, M.; Coppola, E.; Giorgi, F.; da Rocha, R.P.; Cuadra, S.V. 2014. Climate change impact on precipitation for the Amazon and La Plata basins. *Climatic Change*, 125: 111–125.
- Marengo, J.A. 2004. Interdecadal variability and trends of rainfall across the Amazon basin. *Theoretical and Applied Climatology*, 78: 79–96.
- Marengo, J.A.; Chou, S.C.; Kay, G.; Alves, L.M.; Pesquero, J.F.; Soares, W.R.; *et al.* 2012. Development of regional future climate change scenarios in South America using the Eta CPTEC/HadCM3 climate change projections: climatology and regional analyses for the Amazon, São Francisco and the Paraná River basins. *Climate Dynamics*, 38: 1829–1848.
- Marengo, J.A.; Souza, C.M.; Thonicke, K.; Burton, C.; Halladay, K.; Betts, R.A.; *et al.* 2018. Changes in climate and land use over the Amazon Region: Current and future variability and trends. *Frontiers in Earth Science*, 6: 228. doi.org/10.3389/feart.2018.00228
- Mehta, V.M. 1998. Variability of the tropical ocean surface temperatures at decadal–multidecadal timescales. Part I: The Atlantic Ocean. *Journal of Climate*, 11: 2351–2375.
- Mellor, G.L.; Yamada, T. 1974. A Hierarchy of turbulence closure models for planetary boundary layers. *Journal of the Atmospheric Sciences*, 31: 1791–1806.
- Mesinger, F. 1984. A blocking technique for representation of mountains in atmospheric models. *Rivista di Meteorologia Aeronautica*, 44: 195–202.
- Nepstad, D.C.; Moreira, A.G.; Alencar, A.A. 1999. *Floresta em Chamas: Origens, Impactos e Prevenção do Fogo na Amazônia*. IPAM/Programa Piloto para a Proteção das Florestas Tropicais do Brasil, Brasília, 202p.
- Nobre, C.A.; Sellers, P.J.; Shukla, J. 1991. Amazonian deforestation and regional climate change. *Journal of Climate*, 4: 957–988.
- Nobre, C.A.; Borma, L.D.S. 2009. ‘Tipping points’ for the Amazon forest. *Current Opinion in Environmental Sustainability*, 1: 28–36.
- Nobre, P.; Siqueira, L.S.P.; de Almeida, R.A.F.; Malagutti, M.; Giarolla, E.; Castelão, G.P.; *et al.* 2013. Climate Simulation and Change in the Brazilian Climate Model. *Journal of Climate*, 26: 6716–6732.
- Nogueira, J.; Rambal, S.; Barbosa, J.; Mouillot, F. 2017. Spatial pattern of the seasonal drought/burned area relationship across Brazilian biomes: Sensitivity to drought metrics and global remote-sensing fire products. *Climate*, 5: 42. doi.org/10.3390/cli5020042
- Pesquero, J.F.; Chou, S.C.; Nobre, C.A.; Marengo, J.A. 2010. Climate downscaling over South America for 1961–1970 using the Eta Model. *Theoretical and Applied Climatology*, 99: 75–93.
- Reboita, M.S.; Kuki, C.A.C.; Marrafon, V.H.; de Souza, C.A.; Ferreira, G.W.S.; Teodoro, T.; *et al.* 2022. South America climate change revealed through climate indices projected by GCMs and Eta-RCM ensembles. *Climate Dynamics*, 58: 459–485.
- Rocha, V.M.; Correia, F.W.S.; Satyamurty, P.; De Freitas, S.R.; Moreira, D.S.; Da Silva, P.R.T.; *et al.* 2015. Impacts of land cover and greenhouse gas (GHG) concentration changes on the hydrological cycle in Amazon basin: A regional climate model study. *Revista Brasileira de Climatologia*, 15: 7–27.
- Ruiz-Vásquez, M.; Arias, P.A.; Martínez, J.A.; Espinoza, J.C. 2020. Effects of Amazon basin deforestation on regional atmospheric circulation and water vapor transport towards tropical South America. *Climate Dynamics*, 54: 4169–4189.
- Rummukainen, M. 2016. Added value in regional climate modeling. *WIREs Climate Change*, 7: 145–159.
- Saatchi, S.S.; Houghton, R.A.; Dos Santos Alvalá, R.C.; Soares, J.V.; Yu, Y. 2007. Distribution of aboveground live biomass in the Amazon basin: AGLB in the Amazon basin. *Global Change Biology*, 13: 816–837.
- Sekiguchi, M.; Nakajima, T. 2008. A k-distribution-based radiation code and its computational optimization for an atmospheric general circulation model. *Journal of Quantitative Spectroscopy and Radiative Transfer*, 109: 2779–2793.
- Sestini, M.; Alvalá, R.; Mello, E.; Chou, S.; Nobre, C.; Paiva, J.; *et al.* 2002. *Elaboração de Mapas de Vegetação Para Utilização em Modelos Meteorológicos e Hidrológicos*. INPE. (<http://mtc-m12.sid.inpe.br/rep/sid.inpe.br/marciana/2003/03.05.15.05>). Accessed on 16 Jan 2022.
- Silva Junior, C.H.L.; Anderson, L.O.; Silva, A.L.; Almeida, C.T.; Dalagnol, R.; Pletsch, M.A.J.S.; *et al.* 2019. Fire responses to the 2010 and 2015/2016 Amazonian droughts. *Frontiers in Earth Science*, 7: 97. doi:10.3389/feart.2019.00097
- Slingo, J.M. 2007. The development and verification of a cloud prediction scheme for the Ecmwf model. *Quarterly Journal of the Royal Meteorological Society*, 113: 899–927.
- Sombroek, W. 2001. Spatial and temporal patterns of Amazon rainfall: Consequences for the planning of agricultural occupation and the protection of primary forests. *AMBIO*, 30: 388–396.
- Staal, A.; Tuinenburg, O.A.; Bosmans, J.H.C.; Holmgren, M.; van Nes, E.H.; Scheffer, M.; *et al.* 2018. Forest-rainfall cascades buffer against drought across the Amazon. *Nature Climate Change*, 8: 539–543.
- Takata, K.; Emori, S.; Watanabe, T. 2003. Development of the minimal advanced treatments of surface interaction and runoff. *Global and Planetary Change*, 38: 209–222.
- Tarasova, T.A.; Figueroa, S.N.; Barbosa, H.M.J. 2007. Incorporation of new solar radiation scheme into CPTEC GCM. INPE/CPTEC, Cachoeira Paulista, 44 p. (<http://www.fap.if.usp.br/~hbarbosa/uploads/Site/Publications/CliRadTechNote.pdf>). Accessed on 04 Feb 2023.
- Taufik, M.; Setiawan, B.I.; van Lanen, H.A.J. 2015. Modification of a fire drought index for tropical wetland ecosystems by including water table depth. *Agricultural and Forest Meteorology*, 203: 1–10. doi.org/10.1016/j.agrformet.2014.12.006

- Taylor, K.E. 2001. Summarizing multiple aspects of model performance in a single diagram. *Journal of Geophysical Research: Atmospheres*, 106: 7183–7192.
- van Oldenborgh, G.J.; Doblas Reyes, F.J.; Drijfhout, S.S.; Hawkins, E. 2013. Reliability of regional climate model trends. *Environmental Research Letters*, 8: 014055.
- Vogel, M.M.; Hauser, M.; Seneviratne, S.I. 2020. Projected changes in hot, dry and wet extreme events' clusters in CMIP6 multi-model ensemble. *Environmental Research Letters*, 15: 094021.
- Wang, Y.; Leung, L.R.; McGregor, J.L.; Lee, D.-K.; Wang, W.-C.; Ding, Y.; *et al.* 2004. Regional climate modeling: Progress, challenges, and prospects. *Journal of the Meteorological Society of Japan. Ser. II*, 82: 1599–1628.
- Wang, H.; Fu, R. 2007. The influence of Amazon rainfall on the Atlantic ITCZ through convectively coupled Kelvin waves. *Journal of Climate*, 20: 1188–1201.
- Watanabe, M.; Suzuki, T.; O'ishi, R.; Komuro, Y.; Watanabe, S.; Emori, S.; *et al.* 2010. Improved climate simulation by MIROC5: Mean states, variability, and climate sensitivity. *Journal of Climate*, 23: 6312–6335.
- Xue, Y.; Zeng, F.J.; Mitchell, K.E.; Janjic, Z.; Rogers, E. 2001. The impact of land surface processes on simulations of the U.S. hydrological cycle: A case study of the 1993 flood using the SSiB land surface model in the NCEP Eta regional model. *Monthly Weather Review*, 129: 2833–2860.
- Xie, P.; Chen, M.; Shi, W. 2010. CPC unified gauge-based analysis of global daily precipitation. 24th Conf. on Hydrology, Atlanta, GA, Amer. Meteor. Soc. (https://ams.confex.com/ams/90annual/techprogram/paper_163676.htm). Accessed on 04 Feb 2023.
- Xuejie, G.; Zongci, Z.; Yihui, D.; Ronghui, H.; Giorgi, F. 2001. Climate change due to greenhouse effects in China as simulated by a regional climate model. *Advances in Atmospheric Sciences*, 18: 1224–1230.
- Zhao, Q.; Black, T.L.; Baldwin, M.E. 1997. Implementation of the cloud prediction scheme in the Eta model at NCEP. *Weather and Forecasting*, 12: 697–712.

RECEIVED: 24/07/2022

ACCEPTED: 01/01/2023

ASSOCIATE EDITOR: Henrique Barbosa



SUPPLEMENTARY MATERIAL (only available in the electronic version)

Silva *et al.* Regional climate modeling in the Amazon basin to evaluate fire risk

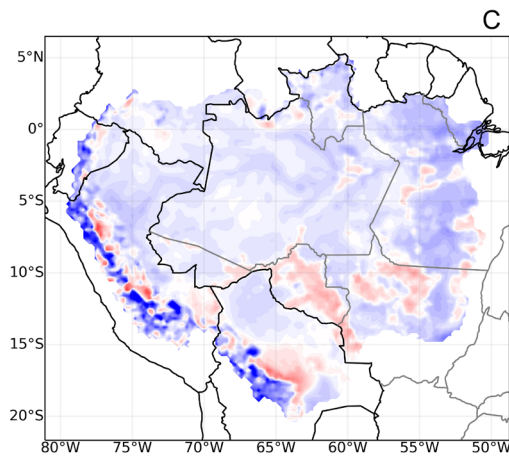
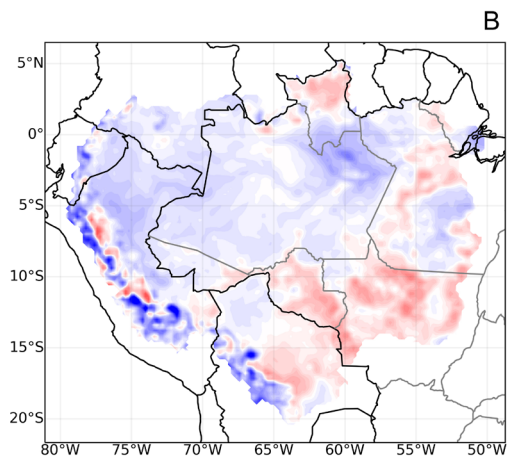
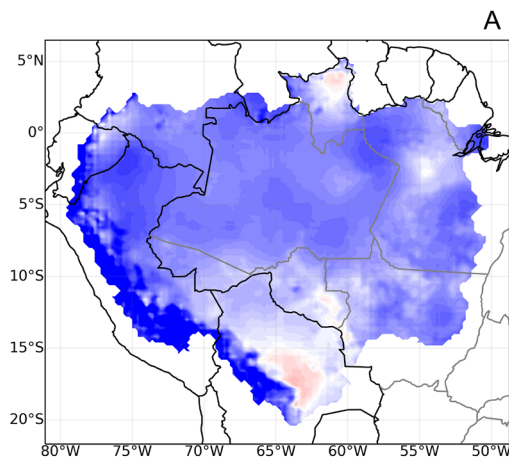


Figure S1. Near-surface temperature bias (°C) for the dry period (July, August, and September) in the Amazon basin from 1979 to 2005 from ERA5 vs. Eta-BESM (A); vs. Eta-HadGEM2-ES (B); and vs. Eta-MIROC5 (C).

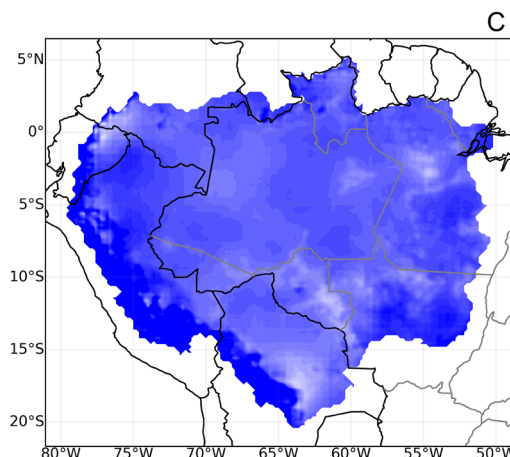
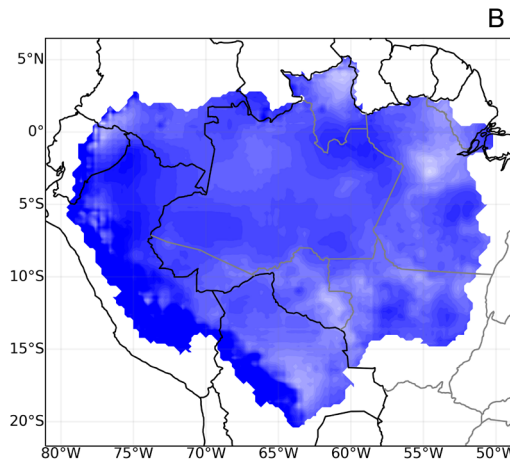
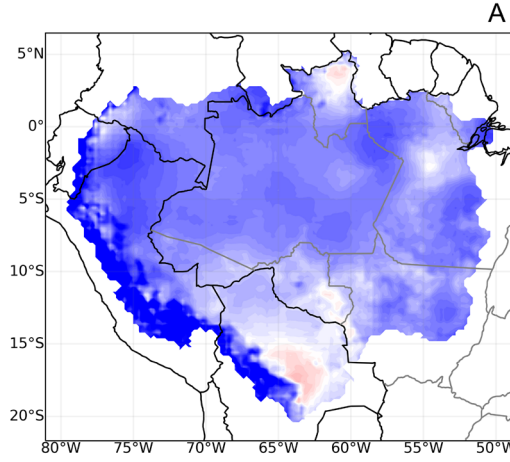


Figure S2. Maximum temperature bias (°C) for the dry period (July, August, and September) in the Amazon basin from 1979 to 2005 from CPC vs. Eta-BESM (A); vs. Eta-HadGEM2-ES (B); and vs. Eta-MIROC5 (C).

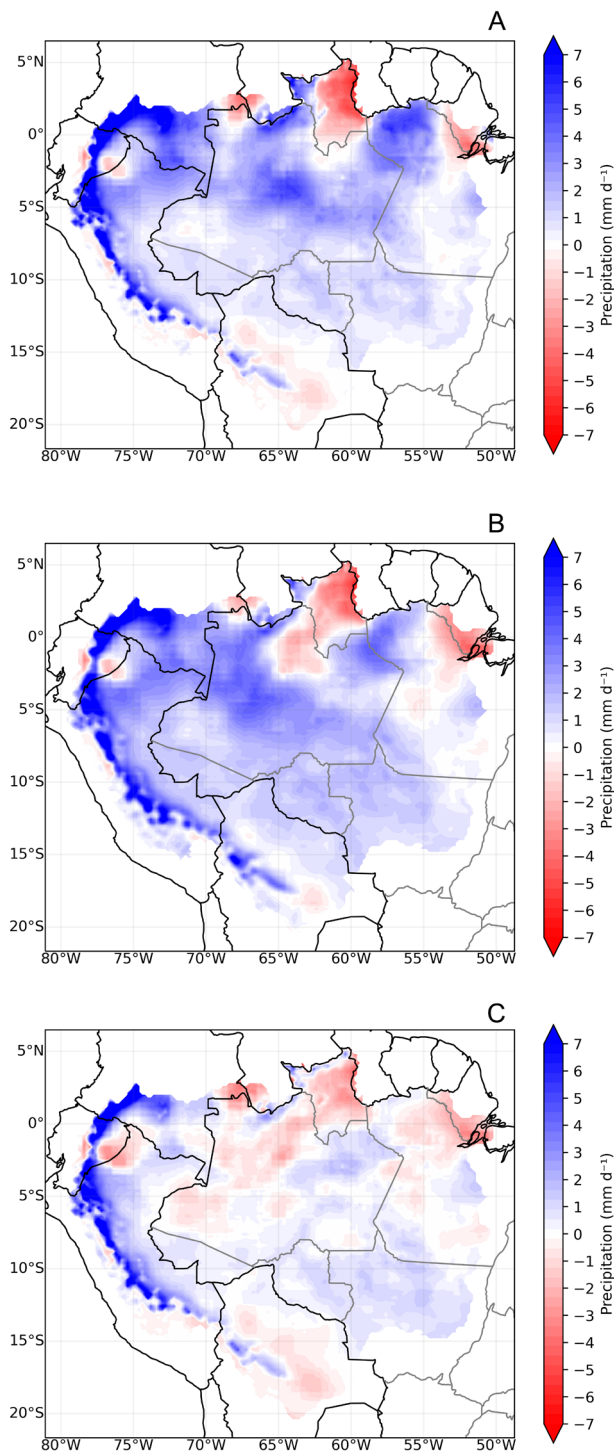


Figure S3. Precipitation bias (mm d^{-1}) for the dry period (July, August, and September) in the Amazon basin from 1979 to 2005 from CPC vs. Eta-BESM (A); vs. Eta-HadGEM2-ES (B); and vs. Eta-MIROC5 (C).

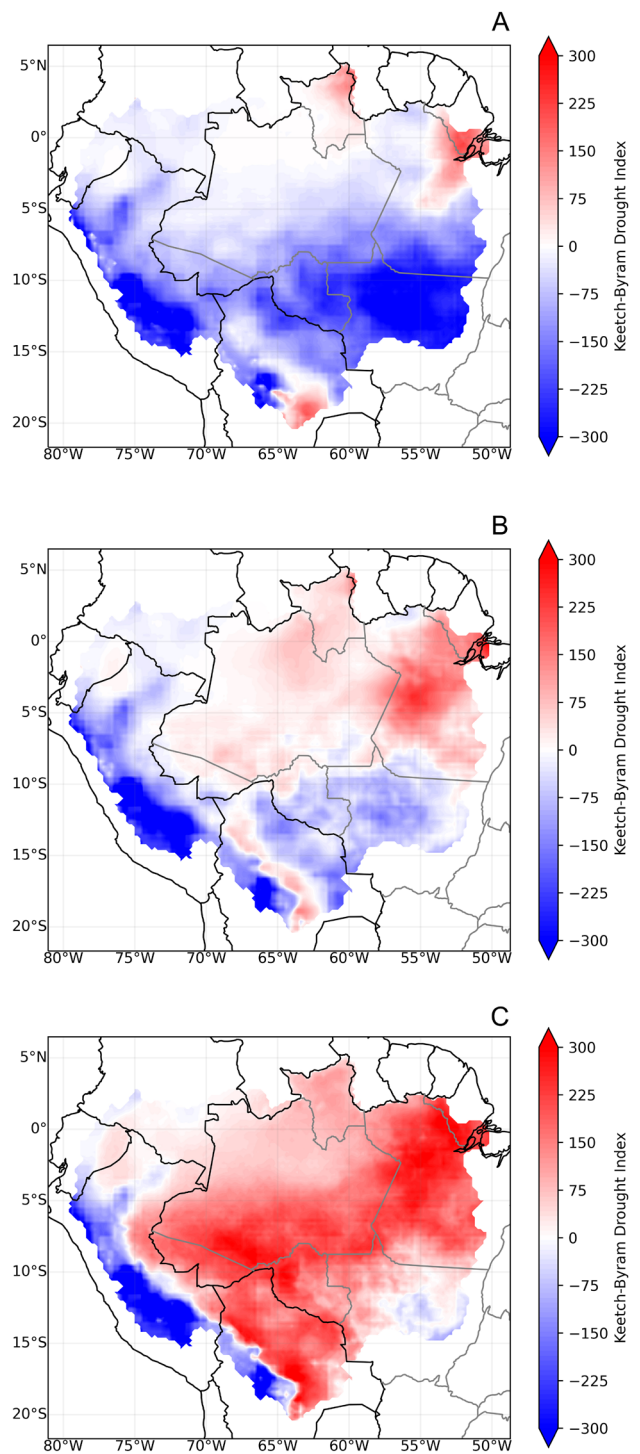


Figure S4. KBDI bias calculated for the dry period (July, August and September) in the Amazon basin from 1979 to 2005 from CPC vs. Eta-BESM data (A); vs. Eta-HadGEM2-ES data (B); and vs. Eta-MIROC5 data (C).